

Quantitative analysis of SCIAMACHY carbon monoxide total column measurements

A. T. J. de Laat,^{1,2} A. M. S. Gloudemans,¹ H. Schrijver,¹ M. M. P. van den Broek,¹
J. F. Meirink,³ I. Aben,¹ and M. Krol^{1,4,5}

Received 19 December 2005; revised 20 February 2006; accepted 27 February 2006; published 7 April 2006.

[1] This paper presents a first quantitative and systematic analysis of one year of SCIAMACHY Carbon Monoxide (CO) total column retrievals from the IMLM algorithm (v6.3) using a chemistry-transport model simulation. The global distribution of modeled and measured CO show similar spatial patterns: a north-south gradient, low CO over mountains, and high CO over emission regions. CO column errors due to instrument noise are closely related to surface albedo and are less than 6% for monthly means at high surface albedo locations, improving to ~1% for ideal circumstances: cloud-free pixels, high surface albedo, and spatial averaging ($3^\circ \times 2^\circ$). Quantitative comparison shows that measured and modeled seasonality agree very well at several locations with different types of seasonal cycles. Differences between SCIAMACHY CO and model results are less than 13% except for regions with large instrument-noise errors. Differences larger than the 2σ instrument-noise error (95% confidence interval) occur in some regions with small noise errors, for example southern Africa. In this case the SCIAMACHY CO variations are different from the model biomass-burning emission seasonal cycle and more in agreement with observed fire count seasonality. The comparison with model results indicates that despite unforeseen time-dependent instrument-calibration complications, SCIAMACHY CO total column retrievals are of sufficient quality to provide useful new information on the global distribution and variation of CO. **Citation:** de Laat, A. T. J., A. M. S. Gloudemans, H. Schrijver, M. M. P. van den Brock, J. F. Meirink, I. Aben, and M. C. Krol (2006), Quantitative analysis of SCIAMACHY carbon monoxide total column measurements, *Geophys. Res. Lett.*, 33, L07807, doi:10.1029/2005GL025530.

1. Introduction

[2] The SCanning Imaging Absorption spectroMeter for Atmospheric CHartography (SCIAMACHY; hereafter referred to as SCIA) on board the ENVISAT satellite allows for the measurement of carbon monoxide (CO). Validation of the retrieved near-infrared SCIA CO total columns (hereafter CO measurements) is difficult for several reasons.

¹Netherlands Institute for Space Research (SRON), Utrecht, Netherlands.

²Now at Royal Dutch Meteorological Institute (KNMI), de Bilt, Netherlands.

³Institute for Marine and Atmospheric Research (IMAU), Utrecht University, Netherlands.

⁴Meteorology and Air Quality Group, Wageningen University, Wageningen, Netherlands.

⁵Formerly at Institute for Marine and Atmospheric Research (IMAU), Utrecht University, Netherlands.

Comparison with MOPITT (Measurements Of Pollutants In The Troposphere) [Deeter *et al.*, 2003] is hampered by different measurement sensitivities to CO at different heights [Buchwitz *et al.*, 2005]. SCIA is uniformly sensitive to the entire troposphere whereas the thermal infrared MOPITT instrument is mostly sensitive to the middle and upper troposphere [Deeter *et al.*, 2004]. Ground-based FTIR measurements provide high quality total column measurements but have very limited spatial coverage [Dils *et al.*, 2005]. Validation with FTIR measurements often consists of comparison with SCIA CO measurements within a range of several hundreds to thousands of kilometers [Sussmann and Buchwitz, 2005; Dils *et al.*, 2005]. As a result, such a validation of SCIA CO is based on very few truly collocated measurements. In addition, some FTIR stations are located on top of mountains which – due to their small spatial footprint – are also difficult to compare with SCIA CO total column measurements which have a footprint of $30 \times 120 \text{ km}^2$. Other complications can be low surface albedo, which enhances SCIA noise errors and clouds, which reduce collocation possibilities [Sussmann and Buchwitz, 2005]. Only qualitative comparisons have been done so far using visual identification of spatial patterns correlating SCIA with MOPITT CO total column measurements or with MODIS fire count maps [Buchwitz *et al.*, 2004, 2005; Frankenberg *et al.*, 2005; De Beek *et al.*, 2006].

[3] Here we take a different approach by using model results from a chemistry-transport model (CTM) as a means of evaluating the SCIA CO measurements. An obvious advantage is that model results are available for every SCIA measurement which allows for a systematic and quantitative evaluation. A disadvantage is that uncertainties in model CO emissions translate into uncertainties in modeled CO. However, CO variations are also strongly influenced by transport pathways and seasonal OH destruction. Seasonal variations in transport and destruction are less uncertain than their day-to-day variations, especially away from emission regions, and are well represented in the model. Moreover, independent surface observations of different tracers have been used to validate the chemistry and transport in the model [Dentener *et al.*, 2003] and show that the model is a useful tool to evaluate seasonal SCIA CO measurements.

2. Retrieval and Calibration

[4] The CO total columns are retrieved from spectra measured by SCIA between 2324.5–2337.9 nm. These near-infrared retrievals are complex due to many instrument/calibration issues described by Gloudemans *et al.*

[2005]. The most important problems are the continuous growth of an ice layer on the detectors and increasing number of dead detector pixels over time due to radiation damage (Q. L. Kleipool, et al., submitted manuscript, 2005). Therefore, the temporal behavior of the retrieved CO columns should be evaluated carefully.

[5] Effects of these instrumental issues have been reduced by applying dedicated in-flight decontamination procedures and additional in-flight calibration measurements, as well as improvements to the calibration [Lichtenberg *et al.*, 2005]. In addition, a correction for the ice layer is applied based on modeled CH₄ columns only [Gloude-mans *et al.*, 2005]. The retrieval results presented here are derived with the Iterative Maximum Likelihood Method (IMLM, v6.3) [Gloude-mans *et al.*, 2005; Straume *et al.*, 2005], which retrieves columns of CO, CH₄ and H₂O simultaneously. For all retrievals the same a-priori CO profile is used which is scaled as a whole to obtain a good fit to the spectrum. The CO total column averaging kernels, computed in the same way as was done by Buchwitz *et al.* [2004], are close to 1 up to ~200 hPa, indicating that changes in the lower troposphere are measured by SCIA. Therefore no averaging kernel is applied to the modeled CO total columns; modeled CO profiles are integrated from the surface to the top model level (1 hPa). The current IMLM v6.3 algorithm contains two major improvements compared to previous versions: the 2004 version of the HITRAN spectroscopic database [Rothman *et al.*, 2005] has been incorporated and temperature and humidity profiles from ECMWF analyses are used rather than climatological profiles.

3. Clouds, Error Filter, and Calculation of Averages

[6] The SCIA CO total column errors due to random instrument noise turn out to be quite large for single measurements—typically 10–100%—and are related to variations in surface albedo and solar zenith angle. Due to these large noise errors multiple single column measurements need to be averaged to obtain information on CO with a useful precision. A common method to average measurements with different errors is to use weighted means. The weight of each measurement is taken inversely proportional to the square of the errors:

$$X_{\text{wav}} = \frac{\sum w_i x_i}{\sum w_i} \quad \text{in which} \quad w_i = \frac{1}{\sigma_i^2}$$

With X_{wav} the weighted average, x_i a single column measurement, σ_i the error corresponding to measurement x_i and w_i the weight of this measurement. The error of the weighted mean (X_{wav}) is expressed as:

$$\sigma_{\text{wav}} = \frac{1}{\sqrt{\sum w_i}}$$

We apply this method to retrieved CO columns – as well as to collocated model values – for both spatial and temporal averaging using the instrument-noise errors.

[7] The measurements need to be filtered to remove a number of biases. Only pixels with a cloud cover of less

than 20% are used. This cloud cover has been determined from the number of cloud-free polarization measurements (7×30 km) within one SCIA ground pixel ($60\text{--}240 \times 30$ km) using the SPICI algorithm [Krijger *et al.*, 2005]. CO column measurements for very low surface albedos (<0.05 ; some locations over land and all above sea) – and thus very low signal-to-noise – often turn out to be unrealistically high with large noise errors ($>1.5 \cdot 10^{18}$ molecules/cm²) and are removed.

[8] We combine retrieved CO columns on a monthly $3^\circ \times 2^\circ$ lon-lat grid, which corresponds to the TM4 model resolution. Because of low land surface albedos, frequent high cloud cover, possible errors at large solar zenith angles at high latitudes, we restrict the analysis to the latitude range of 60°S to 60°N .

4. Model Description

[9] The global chemistry-transport model TM4 [Meirink *et al.*, 2005] used for this study is a follow-up of TM3 [Dentener *et al.*, 2003]. Anthropogenic CO emissions are based on van Aardenne *et al.* [2001], while natural emissions are as given by Houweling *et al.* [1998]. The seasonality of CO biomass emissions is based on the Hao and Liu [1994] estimates. Meteorological ECMWF analysis input fields used in TM4 are pre-processed as described by Bregman *et al.* [2003].

[10] Model results have been compared to CMDL (Climate Monitoring and Diagnostics Laboratory; as of October 2005 Global Monitoring Division) surface CO measurements [Novelli *et al.*, 2003] for the period 2003–2004. Results from this comparison can be found in Figure S1 of the auxiliary material.¹ In general, average CO concentrations as well as long term (monthly) and short term (desseasonalized) variability are adequately reproduced by the model. The model results can thus be used as a powerful tool to evaluate SCIA CO measurements.

5. Results

[11] Figure 1 shows the annual average SCIA measured and TM4 modeled CO total columns for September 2003 to August 2004 (prior to September 2003 measurements are of insufficient quality due to calibration and instrumental issues). A number of similarities can be seen. CO columns are lower over southern South America, southern Africa and over Australia compared to northern mid-latitudes. Emission regions like Amazonia, equatorial Africa (biomass burning), South and Southeast Asia, Europe and North America (anthropogenic) can clearly be discerned, as expected. CO columns are lower over the mountainous regions of the Himalaya, the Middle East, the Andes, and the Rocky Mountains.

[12] Discrepancies are also visible: SCIA CO columns are higher at northern mid-latitudes, over East Asia, Amazonia, Africa southeast of the equator and over Indonesia. On the other hand, measured CO is lower over India and also over Northern Africa ($10^\circ\text{--}30^\circ\text{N}$). Furthermore, the spatial variability in CO columns over low surface albedo

¹Auxiliary material is available at <ftp://ftp.agu.org/apend/gl/2005gl025530>.

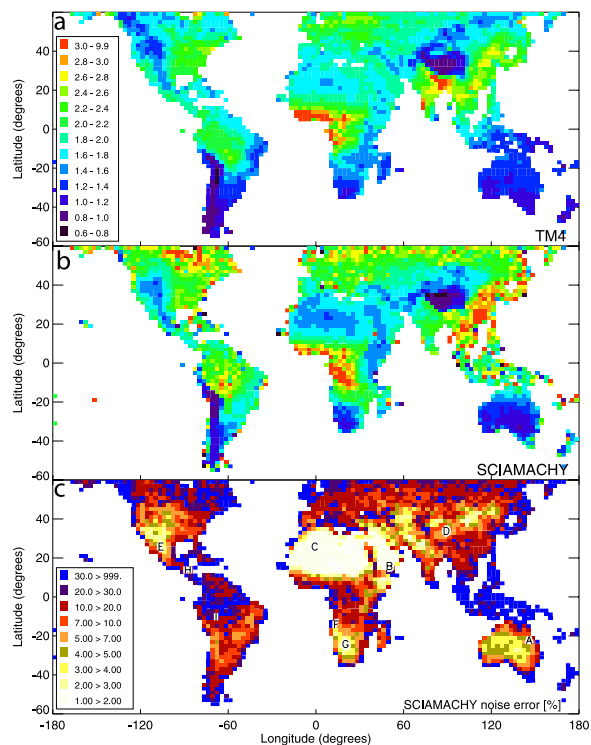


Figure 1. Annual mean CO total columns (10^{18} molecules/ cm^2 ; September 2003–August 2004) on $2^\circ \times 3^\circ$ resolution for (a) TM4 and (b) SCIA. (c) The instrument-noise related SCIA errors (as % of the annual mean TM4 CO total column value). Indicated in Figure 1c are also the locations used in Figure 2.

regions (high latitudes, tropics) is higher in the measurements than in the model results.

[13] Noise errors of the annual mean SCIA CO are shown in Figure 1c. Clearly small errors are obtained for arid regions like deserts, which have a high surface albedo and low cloud cover. Larger errors are found over vegetated regions (tropical rainforests, higher latitudes) and partial sea pixels, reflecting lower surface albedos and more cloudy scenes. Most annual mean CO measurements have noise errors smaller than 10%.

[14] Some discrepancies may also be explained by the inaccurate model emissions. Large forest fires occurred at high latitudes in 2003 (Siberia) [Yurganov *et al.*, 2005] and 2004 (Alaska) and their emissions are not included in the model simulation. Similarly, the climatological biomass burning emissions used in the model over equatorial regions may not be representative for this time period. Current estimates of east Asian CO emissions may be too low [Pétron *et al.*, 2004]. Higher hydrocarbon emission estimates – a strong indirect source of CO, notably isoprene – are also quite uncertain. In addition, model emissions over India may be overestimated (J. van Aardenne, personal communication, 2005).

[15] We further evaluate the measurements by comparing the seasonal variations in CO columns for a selected number of locations (Figure 1c; corresponding statistics are listed in Table S1 of the auxiliary material). Figures 2a–2f measured and modeled seasonal variations agree well. For Australia

(Figure 2a) maximum CO columns values occur around September while minimum values occur around February. Arabia (Figures 2b), Algeria (Figure 2c), and Mexico (Figure 2e) minimum values occur around September while maximum values occur around February. Southern Tibet (Figure 2d) shows relatively constant CO throughout most of the year with significantly higher CO during the Indian summer monsoon, when Indian pollution is transported by convection from the surface to the free troposphere and then further advected away from India, enhancing CO columns over Tibet. Over Angola (Figure 2f) a large peak in CO occurs during July–October in both model results and measurements, which is related to biomass burning emissions from equatorial Africa. Measured and modeled seasonality of CO for all these locations compare quite well, with average absolute differences in monthly means well below 10%. Differences also occur, for example, over Algeria (Figure 2c) during January to May, where modeled CO is higher. This pattern is consistently found over northwestern Africa as suggested by Figure 1 and most likely related to inaccurately modeled biomass burning emission in north-equatorial Africa. Note that Figures 2a–2f have small noise errors (generally less than 6% for monthly means) due to a high surface albedo and sufficient ‘cloud-free’ SCIA measurements per month and grid box. Figures 2h and 2i have lower surface albedos and fewer ‘cloud-free’ observations and thus larger noise errors. For Honduras (Figure 2h) the monthly mean noise errors for January to April are smaller and measurements are close to modeled values. For the other months – as well as for Brazil (Figure 2i) – noise errors are larger (>10%) leading to larger differences with the model results. For most months modeled CO still falls within twice the (1σ) noise error. However, the large errors hamper a comparison of seasonal variations since the measured month-to-month variations are much smaller than individual monthly mean noise errors. For these locations useful information can only be obtained by averaging over larger regions or time periods.

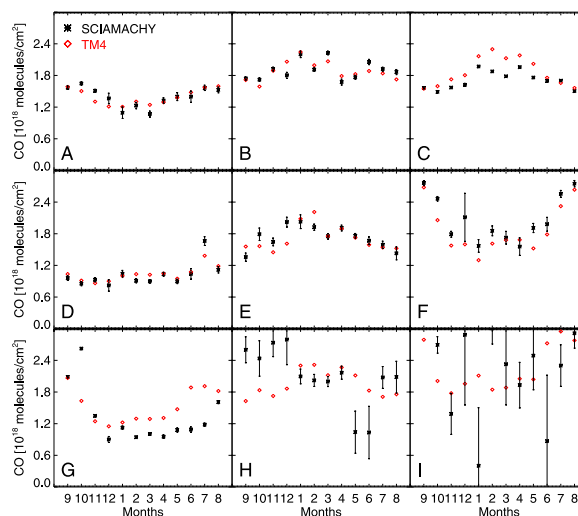


Figure 2. Comparison of monthly mean CO total columns from SCIA (black) and TM4 (red) for nine specific locations ($2^\circ \times 3^\circ$ grid boxes). Error bars denote the SCIA noise error.

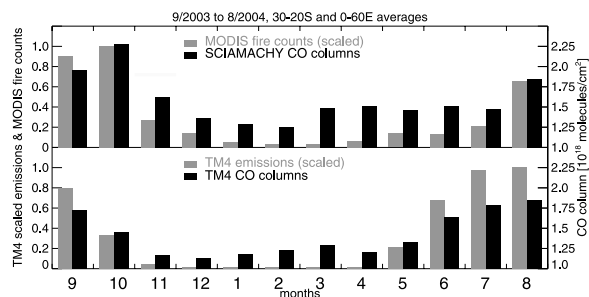


Figure 3. Comparison of monthly mean measured (black, top) and modeled (black, bottom) CO total column values for region between 20° – 30° S and 0° – 60° E. Indicated are also monthly MODIS fire counts and TM4 emissions (grays; scaled with the maximum value for counts and emissions during the 12 months). The MODIS fire counts are obtained from the gridded MODIS monthly fire counts (MOD14CMH [Giglio, 2005]; <http://modis-fire.umd.edu/>).

[16] A remarkable difference is found over South Africa (Figure 2g) where the measurements have small noise errors. A distinct maximum in SCIA CO is seen in September and October 2003 and August 2004. The model results do not show a peak in CO in October 2003 while CO increases after May 2004. Figure 3 shows a comparison of measured and TM4 modeled CO columns averaged over a box between 20° – 30° S and 0° – 60° E including location G. Indicated in the figure are also the model emissions and measured fire counts from MODIS [Giglio, 2005]. The model results clearly show that the enhancement in CO columns over this region is strongly correlated to CO emissions (mainly biomass burning). Modeled CO decreases after September 2003 and increases from June 2004 onward. In contrast, the measurements indicate that CO peaks in September and October 2003 and only increases in August 2004. These observations are well correlated with observed fire counts. Thus, the biomass burning emission climatology used in the TM4 simulation differs in timing from the actual fire counts which are a proxy for emissions. This is a likely cause for the differences in measured and modeled CO columns and highlights the potential use of SCIA CO measurements to optimize surface emissions.

6. Summary

[17] This paper presents a first systematic and quantitative analysis of SCIA total CO column measurements. The noise error of a single SCIA CO total column measurement is quite large (10–100%) but averaging multiple measurements in space ($2^{\circ} \times 3^{\circ}$) and time produces average CO columns that have smaller noise errors. These measurements compare well with model results. For most cases presented the monthly noise errors (1σ) are less than 7% while differences with the model are less than 13%. For ideal cases, for example low cloud cover and high surface albedo, the noise errors of monthly mean CO column measurements can be as low as 1%. In general, differences with the model results are within twice the noise errors (2σ ; 95% confidence level). A pronounced

exception is South Africa where a different biomass burning emission seasonality explains large differences between measurements and model results. This result shows that SCIA observations can be used to evaluate CO emission inventories. In addition, the good time correlation between measured and modeled seasonal variations indicate that the time dependent growth of the ice layer on the SCIA CO channel is well characterized and corrected for.

[18] The near infrared SCIA CO total column measurements are the first satellite measurements with a good sensitivity to the lowest troposphere, which offers good perspectives for future applications like inverse modeling. Furthermore, the SCIA CO measurements are complementary to thermal infrared measurements, for example from MOPITT, which have higher sensitivities to the middle and upper troposphere.

[19] **Acknowledgments.** This research was partly funded by the Netherlands Agency for Aerospace Programmes (NIVR). Data was provided by the European Space Agency (ESA).

References

- Bregman, B., et al. (2003), On the use of mass-conserving wind fields in chemistry-transport models, *Atmos. Chem. Phys.*, 3, 447–457.
- Buchwitz, M., et al. (2004), Global carbon monoxide as retrieved from SCIAMACHY by WFM-DOAS, *Atmos. Chem. Phys.*, 4, 1945–1960.
- Buchwitz, M., et al. (2005), Carbon monoxide, methane and carbon dioxide columns retrieved from SCIAMACHY by WFM-DOAS: Year 2003 initial data set, *Atmos. Chem. Phys. Disc.*, 5, 1943–1971.
- De Beek, R., et al. (2006), Atmospheric carbon gases retrieved from SCIAMACHY by WFM-DOAS: Improved global CO and CH₄ and initial verification of CO₂ over Park Falls (46° N, 90° W), *Atmos. Chem. Phys. Disc.*, 6, 363–399.
- Deeter, M. N., et al. (2003), Operational carbon monoxide retrieval algorithm and selected results for the MOPITT instrument, *J. Geophys. Res.*, 108(D24), 4399, doi:10.1029/2002JD003186.
- Deeter, M. N., L. K. Emmons, D. P. Edwards, J. C. Gille, and J. R. Drummond (2004), Vertical resolution and information content of CO profiles retrieved by MOPITT, *Geophys. Res. Lett.*, 31, L15112, doi:10.1029/2004GL020235.
- Dentener, F., et al. (2003), Trends and inter-annual variability of methane emissions derived from 1979–1993 global CTM simulations, *Atmos. Chem. Phys.*, 3, 73–88.
- Dils, B., et al. (2005), Comparisons between SCIAMACHY and ground-based FTIR data for total columns of CO, CH₄, CO₂ and N₂O, *Atmos. Chem. Phys. Disc.*, 5, 2677–2717.
- Frankenberg, C., U. Platt, and T. Wagner (2005), Retrieval of CO from SCIAMACHY onboard ENVISAT: Detection of strongly polluted areas and seasonal patterns in global CO abundances, *Atmos. Chem. Phys.*, 5, 1639–1644.
- Giglio, L. (2005), MODIS collection 4 active fire product user's guide, Version 2.0, report, Univ. of Maryland, College Park, Md.
- Gloudemans, A. M. S., et al. (2005), The impact of SCIAMACHY near-infrared instrument calibration on CH₄ and CO total columns, *Atmos. Chem. Phys.*, 5, 2369–2383.
- Hao, W. M., and M. Liu (1994), Spatial and temporal distribution of tropical biomass burning, *Global Biogeochem. Cycles*, 8, 495–504.
- Houweling, S., F. Dentener, and J. Lelieveld (1998), The impact of non-methane hydrocarbon compounds on tropospheric photochemistry, *J. Geophys. Res.*, 103, 10,673–10,696.
- Krijger, J. M., I. Aben, and H. Schrijver (2005), Distinction between clouds and ice/snow covered surfaces in the identification of cloud-free observations using SCIAMACHY PMDs, *Atmos. Chem. Phys.*, 5, 2729–2738.
- Lichtenberg, G., et al. (2005), SCIAMACHY Level 1 data: Calibration concept and in-flight calibration, *Atmos. Chem. Phys. Disc.*, 5, 8925–8977.
- Meirink, J. F., H. J. Eskes, and A. P. H. Goede (2005), Sensitivity analysis of methane emissions derived from SCIAMACHY observations through inverse modeling, *Atmos. Chem. Phys. Disc.*, 5, 9405–9445.
- Novelli, P. C., K. A. Masarie, P. M. Lang, B. D. Hall, R. C. Myers, and J. W. Elkins (2003), Reanalysis of tropospheric CO trends: Effects of

- the 1997–1998 wildfires, *J. Geophys. Res.*, *108*(D15), 4464, doi:10.1029/2002JD003031.
- Pétron, G., C. Granier, B. Khattatov, V. Yudin, J. Lamarque, L. Emmons, J. Gille, and D. P. Edwards (2004), Monthly CO surface sources inventory based on the 2000–2001 MOPITT satellite data, *Geophys. Res. Lett.*, *31*, L21107, doi:10.1029/2004GL020560.
- Rothman, L. S., et al. (2005), The HITRAN 2004 molecular spectroscopic database, *J. Quant. Spectrosc. Radiat. Transfer*, *96*, 139–204.
- Straume, A. G., et al. (2005), The global variation of CH₄ and CO as seen by SCIAMACHY, *Adv. Space Res.*, *36*, 821–827.
- Sussmann, R., and M. Buchwitz (2005), Initial validation of ENVISAT/SCIAMACHY columnar CO by FTIR profile retrievals at the Ground-Truthing Station Zugspitze, *Atmos. Chem. Phys.*, *5*, 1497–1503.
- van Aardenne, J. A., F. J. Dentener, J. G. J. Olivier, C. G. M. Klein Goldewijk, and J. Lelieveld (2001), A 1° × 1° resolution data set of historical anthropogenic trace gas emissions for the period 1890–1990, *Global Biogeochem. Cycles*, *15*, 909–928.
- Yurganov, L. N., et al. (2005), Increased Northern Hemispheric carbon monoxide burden in the troposphere in 2002 and 2003 detected from ground and from space, *Atmos. Chem. Phys.*, *5*, 563–573.
-
- I. Aben, A. M. S. Gloudemans, H. Schrijver, and M. M. P. van den Broek, Netherlands Institute for Space Research (SRON), Sorbonnelaan 2, N-3584CA Utrecht, Netherlands.
- A. T. J. de Laat, Royal Dutch Meteorological Institute (KNMI), NL-3730 AE de Bilt, Netherlands. (laatdej@knmi.nl)
- M. Krol and J. F. Meirink, Institute for Marine and Atmospheric Research (IMAU), Utrecht University, Princetonplein 5, N-3584CC Utrecht, Netherlands.